# Serial Assessment of Sympathetic Reinnervation in a Patient with Myocardial Infarction

Yoshiteru Abe, Tetsuro Sugiura, Yutaka Suga, Kazuya Takehana, Hiroshi Kamihata, Masahiro Karakawa, Mituo Inada and Toshiji Iwasaka

*Second Department of Internal Medicine and Department of Radiology, Kansai Medical University, Osaka, Japan*

Resting [$^{123}$I]MIBG and $^{201}$Tl imaging were performed at 2 wk and 4 and 12 mo after successfully reperfused myocardial infarction. Although [$^{123}$I]MIBG uptake of the infarcted segments revealed significant improvement in the early image at 4 mo, delayed image displayed decreased [$^{123}$I]MIBG uptake. However, decreased [$^{123}$I]MIBG uptake of the delayed image became almost uniform at 12 mo. These observations suggest that reinnervation initially occurs in norepinephrine uptake and then in retention ability. On the other hand, a $^{201}$Tl defect remained in the infarcted segments at 12 mo. Thus, reinnervation can occur not only in the peri-infarct area but also in the infarcted area.

**Key Words:** iodine-123-MIBG; myocardial reinnervation; myocardial infarction

**J Nucl Med 1997; 38:457–459**

Myocardial infarction produces sympathetic denervation as well as perfusion abnormalities in the infarcted and peri-infarcted myocardium (*1–4*). However, little is known about the serial changes of these damages after myocardial infarction. Iodine-123-metaiodobenzylguanidine (MIBG) is an analog of norepinephrine and guanethidine and shares the same uptake mechanism as norepinephrine at the sympathetic nerve terminals (*5*). We report on a patient with acute myocardial infarction who demonstrated significant improvement in [$^{123}$I]MIBG uptake not only in the peri-infarcted area but also in the infarcted area.

## CASE REPORT

A 71-yr-old woman (height: 154 cm, weight: 57 kg) suffering from acute myocardial infarction was admitted to our hospital. The patient had no history of previous myocardial infarction. She had several episodes of chest pain in the 24 hr before the onset of myocardial infarction. The patient underwent coronary angiography on admission, which revealed 100% stenosis of the luminal diameter in the left anterior descending artery. Direct percutaneous transluminal coronary angioplasty was performed successfully, showing less than 25% stenosis of the luminal diameter (Fig. 1). Reperfused time was 6 hr from the onset of myocardial infarction. The collateral flow was graded as 3 (*6*). The peak serum creatine kinase concentration was 1694 mg/dl and electrocardiogram showed Q waves in the V1-V4 leads. However, an increase of the R wave in V1-V4 leads was observed at 12 mo. Biplane left ventricular cineangiography was performed on admission and at 12 mo after the onset of myocardial infarction. As illustrated in Figure 2, left ventricular asynergy showed improvement (akinesis to normal) in the anterior and septal walls at 12 mo. Coronary angiogram at 12 mo showed less than 25% stenosis of the luminal diameter in the left anterior descending artery.

Received Apr. 19, 1996; revision accepted Jul. 31, 1996.

For correspondence or reprints contact: Yoshiteru Abe, MD, Cardiovascular Center, Kansai Medical University,10–15-Fumizono-cho, Moriguchi City, Osaka, 570 Japan.

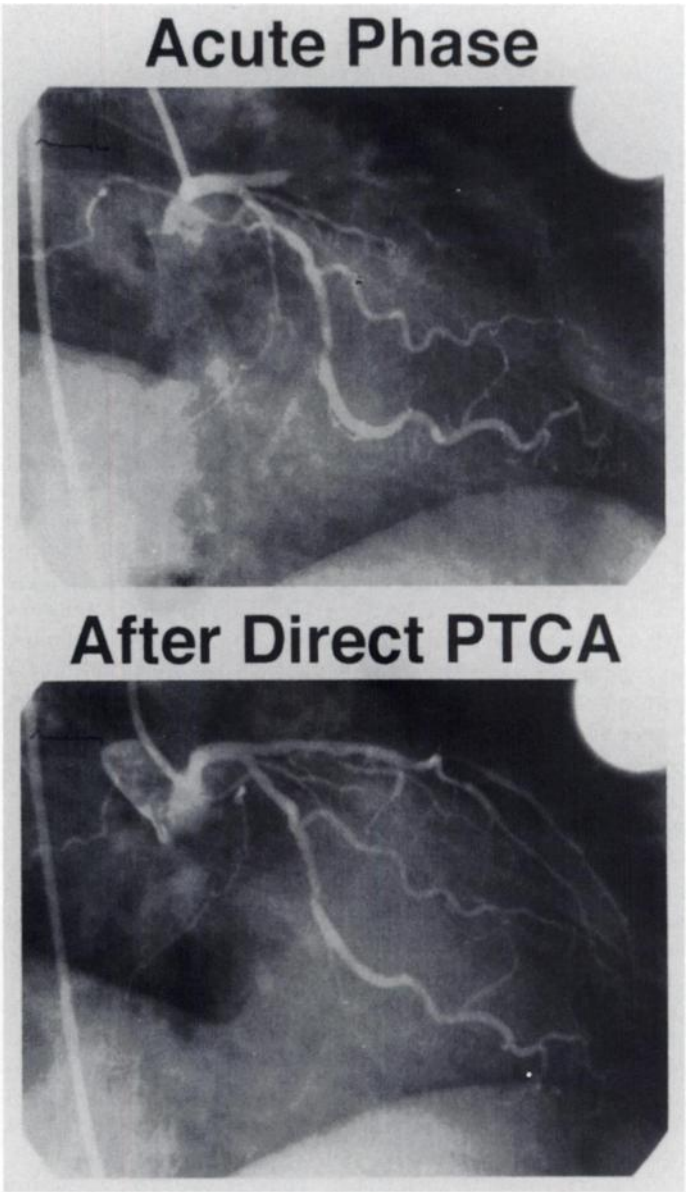


**FIGURE 1.** Coronary angiography before (upper panel) and after percutaneous transluminal angioplasty (lower panel).

### Resting Iodine-123-MIBG and Thallium-201 Scintigraphy

Resting [$^{123}$I]MIBG and $^{201}$Tl imaging were performed at 2 wk and 4 and 12 mo after the onset of myocardial infarction. Each tracer was imaged on a different day and within 2 wk. At rest, 111 MBq [$^{123}$I]MIBG or $^{201}$Tl were injected intravenously, and the patient was imaged with a rotating gamma camera at 15 min and 4 hr postinjection for [$^{123}$I]MIBG and 10 min and 4 hr for $^{201}$Tl. Forty-five projections were obtained over a semicircular 180° arc extending from the 30° right anterior oblique to the 60° left posterior oblique projections. The studies were imaged for 20

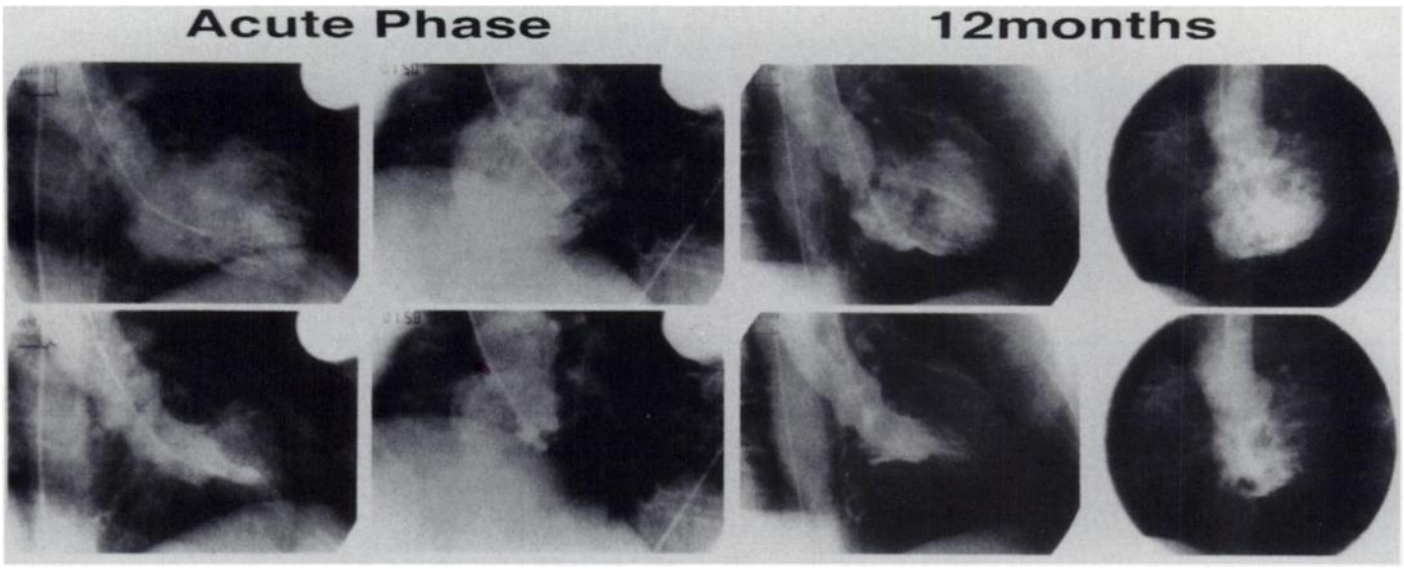


**FIGURE 2.** Left ventriculography before direct percutaneous transluminal angioplasty (left) and 12 mo postinfarction (right).

sec/projection using a 64 × 64 matrix. A large field of view scintillation camera was used, which was equipped with a low-energy, high-resolution, parallel-hole collimator for $^{201}$Tl and a low-energy, general-purpose, parallel-hole collimator for [$^{123}$I]MIBG. For the $^{201}$Tl study, a 30% energy window centered on the 80-keV peak was used, whereas a 20% energy window centered on the 159-keV peak was used for [$^{123}$I]MIBG study. A Butterworth filter (order 5, cutoff frequency 0.15) was used for filtered backprojection. Sagittal and oblique tomograms parallel to the long- and short- axis of the left ventricle were extracted from the filtered transaxial tomograms by performing a coordinate transformation with an appropriate interpolation. No attenuation or scatter correction was used. The imaging procedure was performed by a chief engineer in our laboratory, and selection of tomographic sections were judged by three well-trained radiologists.

### SPECT (Fig. 3)

Two weeks after the onset of myocardial infarction, early $^{201}$Tl image showed decreased activity in the anterior and septal walls with reverse redistribution on the delayed image. Early [$^{123}$I]MIBG image showed decreased activity in the anterior, septal and inferior walls, which were larger than the $^{201}$Tl defects. Furthermore, delayed [$^{123}$I]MIBG image showed further decrease in the activity of the lateral wall compared to the early image.

At 4 mo postinfarction, mild improvement in the anterior and septal wall defects was observed on the early $^{201}$Tl image, and reverse redistribution changed to redistribution. The defect area of the early [$^{123}$I]MIBG image became significantly smaller compared to the $^{201}$Tl defect. However, the delayed image showed decreased [$^{123}$I]MIBG activity in the anterior and septal walls.

At 12 mo postinfarction, the $^{201}$Tl image showed no further improvement in the defect area compared with the 4-mo image. On the other hand, [$^{123}$I]MIBG uptake in the anterior and septal walls on the early and delayed [$^{123}$I]MIBG images became almost uniform.

## DISCUSSION

Although $^{201}$Tl defects persisted 12 mo postinfarction, [$^{123}$I]MIBG uptake in the anterior and septal walls became almost uniform. Because the non-neuronal uptake mechanism is not significant in human myocardium, the improvement observed on the [$^{123}$I]MIBG is considered to be due to the improved neuronal uptake mechanism (*7–8*). Furthermore, the fact that [$^{123}$I]MIBG uptake in the infarcted area improved on the early image before the delayed image (at 4 mo) indicates norepinephrine uptake of the sympathetic nerve terminals can recover before their retention ability.

There is no sympathetic ganglia in the heart, and sympathetic

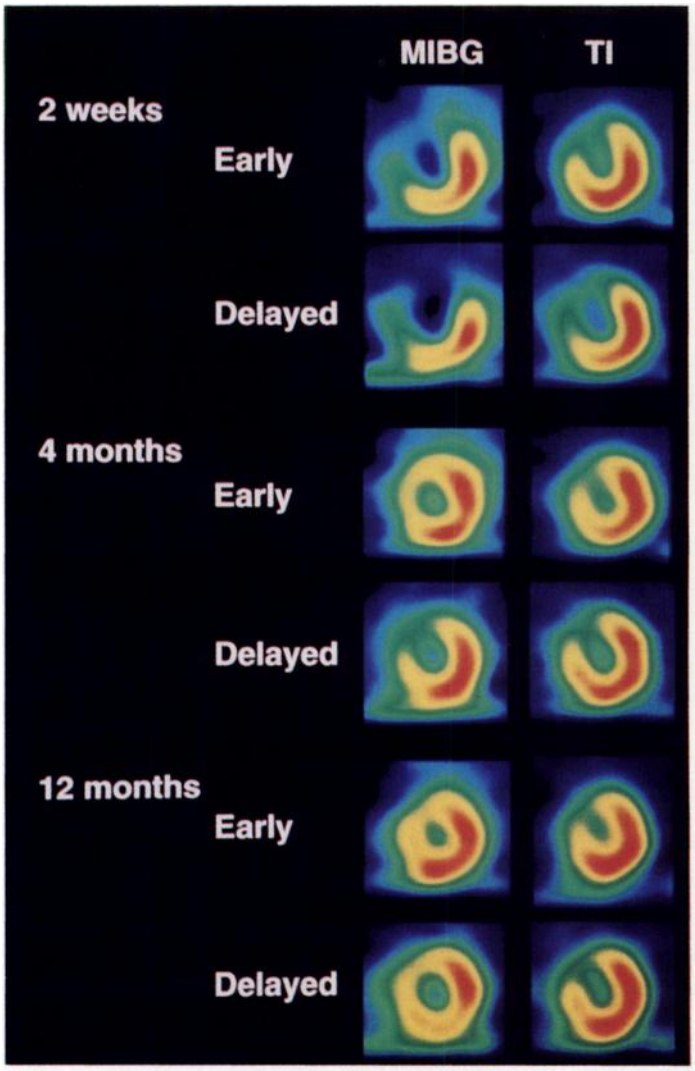


**FIGURE 3.** Serial changes of short-axis slices of [$^{123}$I]MIBG (left) and $^{201}$Tl (right) images from 2 wk to 12 mo postinfarction.

fibers run under the epicardium side of the left ventricular myocardium from base to apex (*2*), which indicate that a subendocardial myocardial infarction that spared the epicardium do not interrupt the sympathetic transmission (*9*). Reinnervation is reported to occur in the peri-infarcted area after transmural myocardial infarction in experimental animal studies and in humans (*1–4*), but there is no report of a reinnervation phenomenon in the infarcted area. The denervation results from interruption of normal neural transmission in postganglionic sympathetic nerve coursing through the area of infarction. However, our patient had good collateral vessels, and successful direct percutaneous transluminal coronary angioplasty was achieved in the early hours of myocardial infarction, which resulted in a relatively small $^{201}$Tl defect size. Left ventricular asynergy of the anterior and septal walls improved, and the electrocardiogram showed increase of R waves in the V1-V4 leads at 12 mo, which suggests the presence of viable myocardium in the infarcted area. Moreover, coronary angiography at 12 mo showed a patent left anterior descending artery. Therefore, one of the causes of reinnervation in our patient was a brief length of sympathetic fiber interruption.

Zipes et al. (*2*) found that preconditioning ischemia preserves the efferent sympathetic response during the first hour of subsequent sustained ischemia. In addition to early reperfusion, repeated episodes of ischemia before the onset of myocardial infarction in our patient could have protected the adrenergic nerve to be more resistant to ischemia. Therefore, initial damage of [$^{123}$I]MIBG uptake after myocardial infarction might have been due to the functional derangements of nerve action rather than the structural damage.

There is less attenuation of 159 keV ($^{123}$I) compared to 80 keV ($^{201}$Tl). Therefore, some of the difference between [$^{123}$I]MIBG and $^{201}$Tl defects at 12 mo may be explained by differential attenuation. However, because $^{201}$Tl defects were in the midportion of the anterior and septal walls, in addition to the patient's small size, indicate that attenuation effects were not significant.

## CONCLUSION

Reinnervation can occur not only in the peri-infarcted area but also in the infarcted area.

## REFERENCES


1. Minardo JD, Tuli MM, Mock BH, et al. Scintigraphic and electrophysiological evidence of canine myocardial sympathetic denervation and reinnervation produced by myocardial infarction or phenol application. *Circulation* 1988;78:1008–1019.
2. Zipes DP. Ischemic modulation of myocardial innervation. *G Ital Cardiol* 1992;22: 615–621.
3. Hartikainen J, Kuikka J, Mäntysaari M, Länsimies E, Pyörälä K. Sympathetic reinnervation after acute myocardial infarction. *Am J Cardiol* 1996;77:5–9.
4. Mitrani R, Burt RW, Klein LS, et al. Regional cardiac sympathetic denervation and reinnervation following myocardial infarction in humans [Abstract]. *Circulation* 1992;86(suppl I):I-247.
5. Kline RC, Swanson DP, Wieland DM, et al. Myocardial imaging in man with I-123-metaiodobenzylguanidine. *J Nucl Med* 1981;22:129–132.
6. Rentrop KP, Cohen M, Blanke H, Phillips RA. Changes in collateral channel filling immediately after controlled coronary artery occlusion by an angioplasty balloon in human subjects. *J Am Coll Cardiol* 1985;5:334–340.
7. Sisson JC, Wieland DM, Sherman P, Mangner TJ, Tobes MC, Jacques S Jr. Metaiodobenzylguanidine as an index of the adrenergic nervous system integrity and function. *J Nucl Med* 1987;28:1620–1624.
8. Dae MW, Marco TD, Botvinick EH, et al. Scintigraphic assessment of MIBG uptake in globally denervated human and canine hearts—implications for clinical studies. *J Nucl Med* 1992;33:1444–1450.
9. Inoue H, Zipes DP. Results of sympathetic denervation in the canine heart: supersensitivity that may be arrhythmogenic. *Circulation* 1987;75:877–887.


# Compartment Model for Measuring Myocardial Oxygen Consumption Using [1-$^{11}$C]Acetate


Karl T. Sun, Kewei Chen, Sung-Cheng Huang, Denis B. Buxton, Herbert W. Hansen, Anatole S. Kim, Stefan Siegel, Yong Choi, Peter Müller, Michael E. Phelps and Heinrich R. Schelbert

*Division of Nuclear Medicine, Department of Molecular and Medical Pharmacology, UCLA School of Medicine; Laboratory of Structural Biology and Molecular Medicine, University of California, Los Angeles, California*



Although [1-$^{11}$C]acetate has been validated as a PET tracer for myocardial oxygen consumption ($MVO_2$) in animals and humans, mono- and biexponential fitting of the tissue time-activity curve yields only estimates of $MVO_2$. This study attempts to develop and validate a simple tracer kinetic model in vivo for estimation of regional $MVO_2$. **Methods:** Twenty-seven experiments were performed in 12 anesthetized dogs with [1-$^{11}$C]acetate and serial PET images under different MBF and $MVO_2$ (baseline, ischemia, xylazine, dobutamine and dipyridamole). Estimates of $MVO_2$ were obtained from dynamic [1-$^{11}$C]acetate PET and model fitting. MBF was measured by radiolabeled microspheres, and $MVO_2$ was calculated by the Fick method using arterial and coronary blood samples. **Results:** The proposed model fitted equally well for all study conditions with a multiple correlation coefficient of 0.985 ± 0.026. Estimated $MVO_2$ correlated linearly with measured $MVO_2$ ($y = 0.033 + 0.690x$, $r = 0.92$, s.e. of estimates = 0.020). **Conclusion:** This study indicates that $MVO_2$ can be assessed with PET and [1-$^{11}$C]acetate over a wide range with a simple tracer kinetic model.



**Key Words:** positron emission tomography; [1-$^{11}$C]acetate; myocardial oxygen consumption

**J Nucl Med 1997; 38:459–466**

Received Nov. 9, 1995; revision accepted July 5, 1996.



For correspondence or reprints contact: Heinrich R. Schelbert, MD, Department of Molecular and Medical Pharmacology, UCLA School of Medicine, Los Angeles, CA 90095.


Carbon-11-acetate has been extensively validated as a PET tracer for the noninvasive assessment of regional myocardial oxidative metabolism (*1–5*). It has been shown that myocardial oxygen consumption ($MVO_2$) can be estimated by either monoexponential fitting of the linear portion or by biexponential fitting of the entire clearance curve of [1-$^{11}$C]acetate clearance (*2*). Although simple, this approach has several potential limitations: (a) only an index of oxidative metabolism, rather than the absolute substrate flux, can be obtained; (b) the distribution of the arterial input function, spillover from myocardium to bloodpool and recirculation of labeled acetate are not taken into account (*6,7*); and (c) estimates are affected by